Few electrons injection in silicon nanocrystals probed by ultrahigh vacuum atomic force microscopy

S. Decossas, J. Vitiello, T. Baron, F. Mazen, S. Gidon

Few electrons injection in silicon nanocrystals probed by ultrahigh vacuum atomic force microscopy

S. Decossas,[a] J. Vitiello, and T. Baron
LTM/CNRS, CEA/Leti/DTS, 17 av. des Martyrs, F-38054 Grenoble, France

F. Mazen
LPM, INSA Lyon, 20 Avenue Albert Einstein, 69621 Villeurbanne Cedex, France

S. Gidon
LICP, CEA/LETI/DOPT, 17 av. des Martyrs, F-38054 Grenoble, France

(Received 22 December 2003; accepted 25 October 2004; published online 13 January 2005)

Ultrahigh vacuum atomic force microscopy has been used to inject and detect charges in individual silicon nanocrystals. The sensitivity of our measurements is shown to be better than 2 e. Injected charge saturates as a function of injection time for a given electric field. The potential of the charged nanocrystal as a function of the number of charges in the dot is in good agreement with a simple electrostatic model. © *2005 American Institute of Physics*. [DOI: 10.1063/1.1829779]

Semiconductor nanocrystals have attracted much attention these last few years for their unique physical properties that could be useful in many applications.[1] Among others, the use of silicon nanocrystals (*nc*-Si) as granular floating gate is very promising for pushing the scaling limit of nonvolatile memories (NVMs)[2] away. Their integration in memory devices has already been shown.[3,4] In such devices, a large number of nanocrystals contribute to the storage of information. To optimize the working parameters of these devices, the understanding of the electrical properties of individual *nc*-Si is needed. Several groups have already shown charge injection and detection in individual nanocrystals[5–7] using atomic force microscopy (AFM) technique. However, in these works, because experiments are performed at atmospheric pressure, sensitivity is not good enough to measure few electrons effects. Moreover, the growth techniques used (SiO_x annealing to precipitate *nc*-Si) do not allow good control of the nanocrystal interface quality and of the surrounding dielectric. In this letter, we present the injection and detection of a controlled number of electrons in individual *nc*-Si produced by low pressure chemical vapor deposition (LPCVD). Both charge injection and detection are performed using an AFM working under ultrahigh vacuum (UHV) condition. Data obtained in these measurements are useful to optimize the working parameter of nanocrystal based NVM that should contain in the future a few *nc*-Si (rather than few hundred today).

Silicon nanocrystals are deposited by silane LPCVD on 10-nm-thick thermal silicon dioxide grown on *p*-type (100) silicon wafer.[8] Their diameter is around 15 nm and their low density ($\approx 10^{10}$ cm^{-2}) allows one to characterize individual *nc*-Si [see Fig. 1(a)]. Charge injection and characterization has been performed on an Omicron AFM working under UHV at a base pressure bellow 2×10^{-10} Torr. We used standard silicon tips coated with a thin layer of $PtIr_5$ with frequency oscillation and radius of curvature given to be around 50 kHz and 15 nm, respectively. To inject charges, the tip is stopped above an *nc*-Si, brought into contact with it thanks to force curve, and a voltage V_{inj} is applied to the sample during a time t_{inj}. Force curves consist of recording the cantilever deflection while the tip-substrate distance Z is swept. It allows us (i) to verify that contact occurs between the tip and the dot during the charging process (positive deflection) and (ii) to estimate the real Z value at which contact occurs (used to estimate quantitatively the number of injected charges). Charge detection is done using electrostatic force microscopy (EFM).[9] With this technique, the AFM tip is retracted in the vertical direction from the surface at a typical distance of 50–100 nm (called lift height) and a voltage of a few volts is applied between the tip and the sample. The AFM tip is then only sensitive to long-range forces such as capacitive or electrostatic ones. In our case, these forces that occur when the tip interacts with the sample are probed by the frequency shift with respect to the tip nominal oscillating frequency. Number of injected charges Q is estimated using the model of Mélin *et al.*[10] and is given by

$$Q = -\frac{\alpha}{g} \times \frac{\varepsilon \,.\, S \,.\, (V_{\mathrm{EFM}} - V_S)}{h} \times R, \tag{1}$$

where α and g are constants describing the tip and nanostructure geometry, respectively, ε is the nanostructure dielectric constant, S its surface, $(V_{\mathrm{EFM}}-V_S)$ the tip-sample voltage, h the lift height, and R the ratio between the measured frequency shift due to electrostatic (i.e., injected charge) and capacitive contribution. This calculation is obtained assuming $R_{nc\text{-Si}}/\varepsilon \ll h$ ($R_{nc\text{-Si}}$ is the radius of the *nc*-Si). In our case, $R_{nc\text{-Si}} \approx 7.5$ nm, $\varepsilon = 11.7$ (for Si) and $h \approx 65$ nm. This equation can then be applied to our system. R is estimated from EFM images [see Fig. 1(b)]. For such an image, the AFM always probes the same line along which it measures electrical properties of both the substrate and one *nc*-Si [dashed line of Fig. 1(a)]. During the image, the EFM voltage V_{EFM} (applied to the sample, the tip being grounded) is modified every 25 lines (there are 400 lines in one image). Horizontal bands on the image 1(b) then correspond to the frequency shift recorded for various V_{EFM} (from −3 V to +4.5 V, with a step of 0.5 V). From such images, we can then compute frequency shift df vs V_{EFM} for both substrate and *nc*-Si (see Fig. 2). From the first image (recorded before any charging of the *nc*-Si), we obtain $df(V_{\mathrm{EFM}})$ for the substrate and the noncharged *nc*-Si, and from each image recorded after charg-

[a]Author to whom correspondence should be addressed; electronic mail: sebastien.decossas@cea.fr

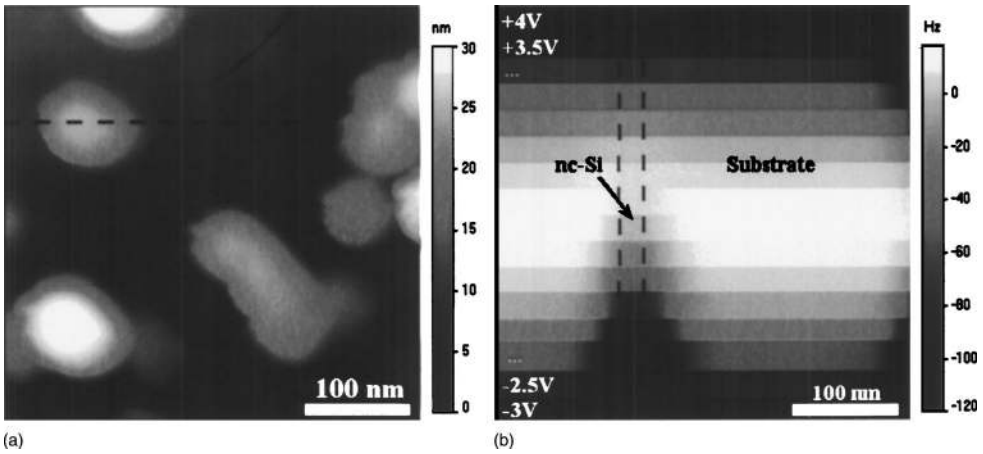

FIG. 1. (a) Noncontact AFM image of *nc*-Si sample. (b) EFM image of one *nc*-Si (numbers indicated on the left part of image (b) are the voltages V_{EFM} used to record the EFM image).

ing, the substrate and the charged *nc*-Si $df(V_{\mathrm{EFM}})$. The ratio R is calculated after each charging following Eq. (2) (Ref. 10)

$$R = \frac{\Delta f_{\mathrm{Charge}} - \Delta f_{\mathrm{Capa}}}{\Delta f_{\mathrm{Capa}}}, \tag{2}$$

where $\Delta f_{\mathrm{charge}} = df_{\mathrm{charged}\ nc\text{-Si}} - df_{\mathrm{noncharged}\ nc\text{-Si}}$ and $\Delta f_{\mathrm{capa}} = df_{\mathrm{noncharged}\ nc\text{-Si}} - df_{\mathrm{substrate}}$ are the frequency shift induced by the electrostatic and capacitive forces, respectively (see Fig. 2). What is called noncharged *nc*-Si corresponds to the initial electrostatic state of the nanocrystal. It is not excluded that charges can already be stored in a *nc*-Si. What we obtain from $df(V_{\mathrm{EFM}})$ measurements and their treatment is then not the total amount of charges that are stored in a *nc*-Si but the number of charges that have been injected in. For nonvolatile memory application, what is important is this number of injected charges, which indeed affects the device threshold voltage. The initial state of the floating gate (*nc*-Si or other media) is a "steady state" which corresponds to the electrostatic equilibrium of the device. The memory effect is driven by the injected charges and not by the number of initial charges.[11] We have developed our own software to extract $df(V_{\mathrm{EFM}})$ curves from EFM images. The standard deviation on df for one point of the curve is lower than 2 Hz. Error bars on $df(V_{\mathrm{EFM}})$ are not represented on curves because errors are too low to be seen. From $df(V_{\mathrm{EFM}})$ curves, we can (i) extract the R ratio, and then determine the quantity of charges that are stored in the *nc*-Si, and (ii) measure the potential of both the *nc*-Si $V_{nc\text{-Si}}$ and the substrate V_{sub}. When the tip and the sample are at the same potential, the interacting force felt by the tip is minimized because there is no electric contribution. On $df(V)$ curve, that corresponds to the highest value of df (since df decreases when the force increases). Moreover, V_{EFM} is applied to the sample, the tip being grounded. The potential $V_{nc\text{-Si}}$ (or V_{sub}) is then equal to $-V_{\mathrm{EFM}}$ for which the derivative of $df(V_{\mathrm{EFM}})$ is null.

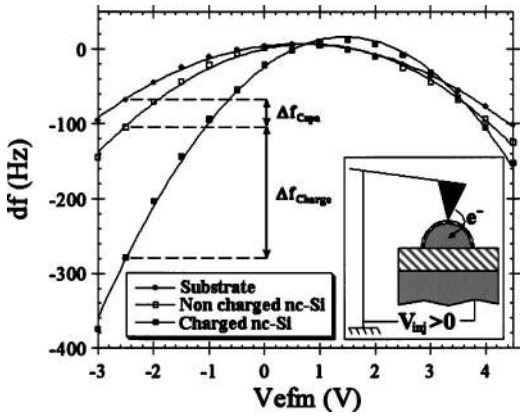

FIG. 2. Frequency shift as a function of the EFM voltage V_{EFM} measured on the substrate (filled circle), the noncharged *nc*-Si (empty square), and the charged *nc*-Si (filled square, $V_{\mathrm{inj}}=4$ V, $t_{\mathrm{inj}}=4$ ms). Lines are second degree polynomial fit of experimental data. These three curves are extracted from the EFM image 1(b). (Inset) Schematic view of charge transfer for positive value of injection potential V_{inj}.

Charging presented in Fig. 2 has been done at $V_{\mathrm{inj}} = +4$ V during $t_{\mathrm{inj}}=4$ ms. For negative values of V_{EFM}, df is minimized once the *nc*-Si is charged (i.e., the interacting force is increased for $V_{\mathrm{EFM}}<0$). For negative values of V_{EFM}, negative charges are brought at the Si/SiO_2 interface. The increasing of the interaction force corresponds to a larger number of charges that create this force. Then, in that condition of charge injection ($V_{\mathrm{inj}}>0$), electrons are stored in the *nc*-Si (as expected, see schematic drawing of Fig. 2).

Figure 3(a) shows the number of charges Q that have been injected in an individual *nc*-Si, 15 nm in diameter. Several injection events are represented on the curve. Injection time t_{inj} (during which the tip is in contact with the dot while the injection voltage is applied to the sample) is set to 50 μs (except for the first event: 100 μs) and injection voltage V_{inj} to 4 V (applied to the sample, the tip being grounded). The potential of the *nc*-Si $V_{nc\text{-Si}}$ is taken into account to set this voltage (i.e., $V_{\mathrm{inj}} - V_{nc\text{-Si}} = 4$ V, we inject charges at a constant electric field). Each point of the curve has been calculated using the method described above. As we can see in Fig. 3(a), number of injected charges saturates at about 12 e after 4 ms. We have observed by working with various tips on various *nc*-Si that saturation time can significantly vary (between 1 and 50 ms). This is certainly due to the *RC* factor of the tip/*nc*-Si contact which is highly dependent on the charging parameters (quality of the tip metallic coating, tip radius of curvature, pressure exerted during contact,…). Notice that using the same parameters and notably $V_{\mathrm{inj}}=4$ V, we did not manage to inject charges in the SiO_2 layer. Moreover, on EFM images, charges are clearly located on *nc*-Si. It ensures that injected charges are related to the *nc*-Si and not to the underlying dielectric layer. We cannot say, however, if they correspond to interface or internal state charges. To quantify Q with Eq. (1) we have to know α, ε, S, and h. The tip geometry is described by α (Ref. 12) following the law $df = A \cdot z^{-\alpha}$. We experimentally checked by performing force-distance curves $df(z)$ for various tip sample voltages that α

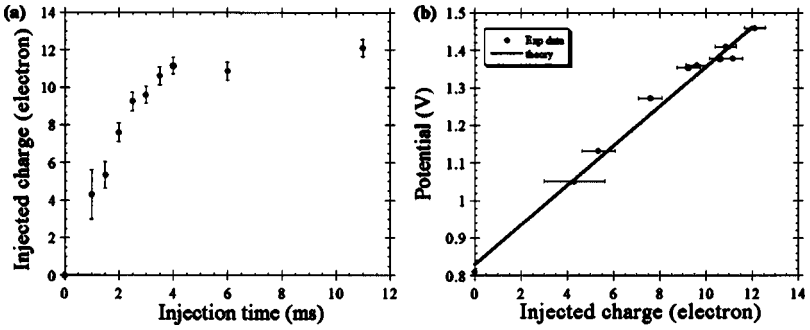

FIG. 3. (a) Charge vs injection time in a *nc*-Si (15 nm in diameter) for an injection voltage of 4 V. (b) Potential of the charged *nc*-Si vs the number of charge.

=1.5. Numerical calculation shows that $g=9/8$ for a hemispherical nanoparticle.[10] It corresponds to what we observe for the geometry of the *nc*-Si we used.[8] Lift height h is measured from force curves performed to contact the *nc*-Si ($\approx$65 nm). We used $\varepsilon=11.7\ \varepsilon_0$ (for silicon) and $S=2\pi\times7.5^2$ nm^2 (surface of a hemispherical particle, 15 nm in diameter). Eventual error on these parameters would change the absolute scale of Q. However, it would not affect the shape of the curve (i.e., the ratio between two measurements of Q) if these parameters do not change during measurements (notably, we checked that the tip geometry does not changed by performing standard topographical images). Error bars plotted on Fig. 2 are calculated taking into account all the parameters of Eq. (1) (see Ref. 13). Main error is due to the determination of R. The calculation of ΔR is inversely proportional to both differences in df signal between (i) noncharged *nc*-Si and substrate (Δf_{Capa}) and (ii) charged *nc*-Si and noncharged *nc*-Si ($\Delta f_{\mathrm{Charge}}$) [see Eq. (2)]. The first difference remains the same for the calculation of all the points of the curve (this is the reference, extracted from the first EFM image). The second one has to be calculated for each point. For a low number of charges in the *nc*-Si, $df(V_{\mathrm{EFM}})$ curves are very similar for charged and noncharged *nc*-Si. Consequently, error is increased. It explains why error bars are larger for low numbers of injected charges. Errors are lower than 1 e for number of injected charges greater than 6 e.

Injected charge of Fig. 3(a) has been determined using measurements performed at $V_{\mathrm{EFM}}=-2$ V. For EFM voltage close to surface potential, errors are large since the measured frequency shifts for both the substrate and the noncharged *nc*-Si are almost the same. For large V_{EFM} (i.e., close to -3 V), interaction force between the tip and the sample becomes important. That may lead to a large static deflection of the cantilever and then can cause the tip/surface distance to be reduced consequently. The hypothesis $R_{nc\text{-Si}}/\varepsilon \ll h$ could not be respected anymore. As a matter of fact, we have already observed $df(V_{\mathrm{EFM}})$ curves that clearly deviate from parabolic shape for large values of V_{EFM}. Charge determination performed for various intermediate V_{EFM} values (typically between -2.5 and -1 V) leads to results that are identical within a margin of 5%.

Finally, we did not observe any discharge of the *nc*-Si for 24 h. This is predictable since (i) *nc*-Si rest on 10-nm-thick SiO_2 and (ii) the tip never contacts the *nc*-Si during measurements.

Figure 3(b) presents the *nc*-Si potential, extracted from $df(V)$ measurements (see Fig. 2), as a function of the charges injected into the *nc*-Si. Making the assumption that the *nc*-Si is a hemispherical volume, we can use the Gauss theorem (i.e., the flux of the electric field E equals the charge in the volume) to determine its potential. After integration of E, we obtain the equation $V_{\mathrm{dot}}=q/(2\pi\varepsilon\varepsilon_0 d)$, where q, ε, and d are the number of charge, the relative dielectric constant, and the diameter of the particle, respectively. Despite the fact that q is an integer, theoretical calculation is represented as a line of Fig. 3 for a better comparison between calculation and experiments. Empty *nc*-Si potential for calculation is set such as it fits with what we have measured. The substrate potential is not supposed to change for various measurements. This is what we observed since we measured a mean value $V_{\mathrm{sub}}=-0.62$ V with a standard deviation lower than 20 mV. We assume the same errors for the determination of the *nc*-Si potential (we then did not plot the potential error bars since they would not be distinguishable). Agreement between experimental work and calculation is pretty good.

We have pointed out injection of charges in an individual *nc*-Si and their detection by electrostatic force microscopy. It is shown that the number of injected charges saturates at 12 for a 15 nm in diameter silicon nanocrystal, using an injection voltage of 4 V. The internal potential of a charged *nc*-Si as a function of the number of charges inside the *nc*-Si is in good agreement with a simple electrostatic model. From experiments and calculation, we estimate the sensitivity of our measurements to be better than 2 e. These measurements will be extended in the near future to check the effect of the nanocrystal size on the charge number at saturation and to another kind of nanocrystal (germanium).

[1] *Handbook of Nanostructure Materials*, edited by H. S. Nalwa (Academic, New York, 2000).
[2] J. DeBlauwe, IEEE Trans. Nanotechnol. **1**, 72 (2003).
[3] S. Tiwari, F. Rana, H. Hanafi, A. Hartstein, E. F. Crabbé, and K. Chan, Appl. Phys. Lett. **68**, 1377 (1996).
[4] B. De Salvo, G. Ghibaudo, G. Pananakakis, P. Masson, T. Baron, N. Buffet, A. Fernandes, and B. Guillaumot, IEEE Trans. Electron Devices **48**, 1789 (2001).
[5] E. A. Boer, M. L. Brongersma, H. A. Atwater, R. C. Flagan, and L. D. Bell, Appl. Phys. Lett. **79**, 791 (2001).
[6] C. Guillemot, P. Budau, J. Chevrier, F. Marchi, F. Comin, C. Alandi, F. Bertin, N. Buffet, C. Wyon, and P. Mur, Europhys. Lett. **59**, 566 (2002).
[7] T. Mélin, D. Deresmes, and D. Stiévenard, Appl. Phys. Lett. **81**, 5054 (2002).
[8] T. Baron, F. Martin, P. Mur, C. Wyon, and M. Dupuy, J. Cryst. Growth **209**, 1004 (2000).
[9] Y. Martin, C. C. Williams, and H. K. Wickramasinghe, J. Appl. Phys. **61**, 4723 (1987).
[10] T. Mélin, H. Diesinger, D. Deresme, and D. Stiévenard, Phys. Rev. B **69**, 035321 (2004).
[11] B. De Salvo, G. Ghibaudo, G. Pananakakis, P. Masson, T. Baron, N. Buffet, A. Fernandes, and B. Guillaumot, IEEE Trans. Electron Devices **48**, 1789 (2001).
[12] T. D. Krauss and L. E. Brus, Phys. Rev. Lett. **83**, 4840 (1999).
[13] We used $\Delta\alpha=0.1$, $\Delta g=0$, $\Delta d_{nc\text{-Si}}$ (for ΔS calculation)$=0.1$ nm, $\Delta V_S=0.02$ V, and $\Delta h=0.1$ nm.